Marine Environmental Research
July 2021, Volume 169 Pages 105380 (9p.)
https://doi.org/10.1016/j.marenvres.2021.105380
https://archimer.ifremer.fr/doc/00699/81097/

Impacts of ocean acidification on growth and toxin content of the marine diatoms *Pseudo-nitzschia australis* and *P. fraudulenta*

Ayache Nour [1, *], Lundholm Nina [2], Gai Frederik [2], Herve Fabienne [1], Amzil Zouher [1], Caruana Amandine [1]

[1] Institut Francaise de Recherche pour L'Exploitation de La Mer: Ifremer, Phycotoxin Laboratory, F-44311, Nantes, France
[2] Natural History Museum of Denmark, University of Copenhagen, Øster Farimagsgade 5, 1307, Copenhagen, Denmark

* Corresponding author : Ayache Nour, email address : ayache.nour@gmail.com

Abstract :

This paper present the effects of ocean acidification on growth and domoic acid (DA) content of several strains of the toxic Pseudo-nitzschia australis and the non-toxic P. fraudulenta. Three strains of each species (plus two subclones of P. australis) were acclimated and grown in semi-continuous cultures at three pH levels: 8.07, 7.77, and 7.40, in order to simulate changes of seawater pH from present to plausible future levels. Our results showed that lowering pH from current level (8.07) to predicted pH level in 2100 (7.77) did not affect the mean growth rates of some of the P. australis strains (FR-PAU-17 and L3-100), but affected other strains either negatively (L3-30) or positively (L3.4). However, the growth rates significantly decreased with pH lowered to 7.40 (by 13% for L3-100, 43% for L3-30 and 16% for IFR-PAU-17 compared to the rates at pH 8.07). In contrast, growth rates of the non-toxic P. fraudulenta strains were not affected by pH changing from 8.07 to 7.40.

The P. australis strains produced DA at all pH levels tested, and the highest particulate DA concentration normalized to cell abundance (pDA) was found at pH 8.07. Total DA content (pDA and dissolved DA) was significantly higher at current pH (8.07) compared to pH (7.77), exept for one strain (L 3.4) where no difference was found. At lower pH levels 7.77–7.40, total DA content was similar, except for strains IFR-PAU-17 and L3-100 which had the lowest content at the pH 7.77. The diversity in the responses in growth and DA content highlights the inter- and intra-specific variation in Pseudo-nitzschia species in response to ocean acidification. When exploring environmental responses of Pseudo-nitzschia using cultured cells, not only strain-specific variation but also culturing history should be taken into consideration, as the light levels under which the subclones were cultured, afterwards affected both maximum growth rates and DA content.

Highlights

► *P. fraudulenta* and *P. australis* strains were able to acclimate and maintain high growth rates at current pH (8.07) and projected pH in 2100 (7.77) compared to the lowest pH level (7.40) ► Domoic acid content was significantly higher for all *P. australis* toxic strains acclimated at the ambient pH level (8.07), and lowest at pH (7.77) ► Strong inter- and intra-specific variation related to the geographical area and the culturing history of *Pseudo-nitzschia* strains

Keywords : Amnesic shellfish poisoning, Domoic acid, Harmful algae, Ocean acidification, Pseudo-nitzschia

1.1 Introduction

Carbon dioxide (CO_2) concentration in the atmosphere increased from 278 ppm to 400 ppm during the pre-industrial period and is predicted to reach between 800 and 1000 ppm by the end of the 21st century (IPCC, 2014; Le Quéré et al., 2018). As atmospheric CO_2 concentrations continue to increase, the amount of dissolved CO_2 in the ocean will also increase and thus oceanic pH will decrease. Oceanic pH has already decreased by 0.1 unit (from on average 8.21 to 8.1) since the beginning of the industrial era, and atmospheric CO_2 is projected to increase and reach about 720-1,020 ppm by the year 2100, which corresponds to a decrease in ocean surface pH by 0.14-0.32 pH units (IPCC, 2014). In addition, coastal and estuarine ecosystems are naturally exposed to pH fluctuations due to upwelling, water depth, tidal currents, residence time, photosynthesis and respiration of phytoplankton (Feely et al., 2008; Middelboe and Hansen, 2007). This acidification may have a significant impact on physiology, proliferation and distribution of phytoplankton species in marine ecosystems (Orr et al., 2005). In addition, changes in pH/pCO_2 can have serious consequences for the functioning of marine ecosystems, from direct effects on physiological responses of phytoplankton and zooplankton (Cornwall et al., 2013; Flynn et al., 2015; Kroeker et al., 2013), to more indirect effects on food web and species interactions (Orr et al., 2005). Ocean acidification (OA) may also affect the distribution of

54 phytoplankton, allowing certain species, mainly diatoms, with an efficient carbon concentrating
55 mechanism (CCM), to thrive and dominate the marine ecosystems (Rost et al., 2008; Trimborn et
56 al., 2013). Apart from ocean acidification, enhanced nutrient release from land may also result in
57 enhancing the development of large phytoplankton blooms (of both harmful algal species HABs
58 and non-HABs) and their eventual bacterial decomposition and resultant release of dissolved
59 carbon dioxide and pH decline (Doney, 2010). Climate change-induced ocean acidification and
60 eutrophication may therefore result in a larger increase in HAB bloom biomass, as blooms will
61 initiate at a lower average pH and thus delay the detrimental effects of high pH at bloom
62 maximum (Flynn et al., 2015; Hansen et al., 2007; Lundholm et al., 2004). Several factors are
63 thus in play when discussing the effect of lowered pH/increased DIC availability on HAB
64 species, making it relevant, but not easy, to explore the effect of lowered pH/increased DIC
65 availability on HAB species. Additional impacts by other biotic and abiotic factors like grazers
66 and temperature will also affect the bloom biomass attained. Specific effects of ocean
67 acidification will depend on the physiology of the individual species (Flynn et al., 2015, 2012) as
68 well as any potential physiological variation within a species.

69 The diatom *Pseudo-nitzschia* species are common and abundant members of coastal
70 phytoplankton communities (Malviya et al., 2016; Trainer et al., 2012). Several species of
71 *Pseudo-nitzschia* produce the neurotoxin, domoic acid (DA), which can cause serious ecological,
72 economic, and health-related problems and are responsible for amnesic shellfish poisoning (ASP)
73 in humans world-wide (Bates et al., 2018). In recent decades, numerous reports have linked
74 mortality events of sea birds, fish and sea mammals to the presence of toxic *Pseudo-nitzschia*
75 blooms and the accumulation of high DA concentrations in these organisms (Goldstein et al.,

2008; Lefebvre et al., 2012; Scholin et al., 2000). In 2015, a long-lasting geographically extensive bloom of the highly toxic species, *P. australis*, was recorded along the North American west coast causing prolonged closures of shellfish harvesting areas and contributing to the illness and death of seabirds and marine mammals (Di Liberto, 2015; McCabe et al., 2016). As anthropogenic CO_2 emissions continue to increase, it is thus important to understand how growth as well as DA production of *Pseudo-nitzschia* species respond to the ongoing changes in the marine environment (i.e., acidification).

In general, acidification has been hypothesized to stimulate primary production of phytoplankton (Riebesell et al., 2007; Rost et al., 2008; Schippers et al., 2004a). Presently, relatively few laboratory studies have examined the effect of lowered pH and increased pCO_2 on the physiology of *Pseudo-nitzschia* species. The findings published show diverging results with respect to growth and DA production in different *Pseudo-nitzschia* species. Studies on *P. fraudulenta* and *P. multiseries* demonstrate significantly increased growth rates with acidification, and significant increase in DA content with increasing CO_2 concentration especially under nutrient-limiting conditions (Sun et al. 2011 and Tatters et al. 2012). Moreover, Wingert (2017) showed an increase in DA cellular content in a single *P. australis* strain due to acidification, whereas the growth rates in contrast to previous studies were not affected until reaching pH 7.8. In addition, Tatters et al. (2018) found that warming and acidification interactions generally increased the cell normalized DA content in *P. multisersie*s in a mixed, natural assemblage. In recent results of a mesocosm experiment conducted in Gullmar Fjord, Sweden, the authors also observed significantly higher particulate DA contents per litre with elevated pCO_2 (OA), here also

97 associated with macronutrient limitation (Wohlrab et al., 2020). Thus, OA apprears to generally
98 increase the production of DA under nutrients limited conditions.

99 The development of high biomass phytoplankton blooms results in lower concentrations of
100 dissolved CO_2 (basification) leading to reduced cellular growth rates in some *Pseudo-nitzschia*
101 species (Lundholm et al., 2004). A decrease in growth rate and simultaneously an increase in DA
102 content was seen in *P. multiseries* grown at elevated pH levels (pH 8.9) compared to pH 7.9 and
103 8.4 (Lundholm et al., 2004; Trimborn et al., 2008). In contrast, no change in the specific growth
104 rates were observed in *P. multiseries* and *P. pungens* when maintained under a wide range of pH
105 (from 5 to 9) (Cho et al., 2001). Overall, these apparently contradicting results might be
106 explained by differences in pH levels, differences among *Pseudo-nitzschia* species, as well as
107 different experimental protocols employed (batch and semi-continuous cultures). Most of the
108 existing studies investigating the effect of changing pH on the physiology and DA production by
109 *Pseudo-nitzschia* species used only one strain as representative of a species. Considering the
110 genetic variability of *Pseudo-nitzschia* species (Bates et al., 2018), it is important to study several
111 strains of each species in order to understand the tolerance and toxin production capacity of
112 *Pseudo-nitzschia* species in response to future ocean acidification.

113 In the present study, we examined the effects of lowered pH on growth and DA content in
114 acclimated strains of *P. australis* and *P. fraudulenta* under nutrient replete conditions. The aim
115 was to evaluate the impact of acidification from present (pH 8.07) to probable future levels (pH
116 7.77 and 7.40) in three different strains of two different *Pseudo-nitzschia* species to understand
117 the isolated effects of lowered pH and increased CO_2. *P. australis* and *P. fraudulenta* are

common and globally widespread species, with *P. australis* being a highly toxic species, and *P. fraudulenta* a non-toxic or very slightly toxic species.

1.2 Materials and methods

Cultures and culture conditions

Six monoclonal strains of *Pseudo-nitzschia* were included, three *P. fraudulenta* strains (PNfra167, PNfra169 and IFR-FRA-17) as non-toxic representatives, and three *P. australis* strains (IFR-PAU-17, L3.4 and L3) as toxin-producing strains. Before the experiments, two subclones, L3-30 and L3-100 were established from the same monoclonal culture (L3), which was split and grown at two different culture conditions for at least 3 months: L3-100 was kept at 100 µmol photons m^{-2} s^{-1} cool white light, while L3-30 was kept at 30 µmol photons m^{-2} s^{-1} cool white light (cool-white fluorescent light, Osram, Germany). The six studied strains were isolated from different geographical regions (France and Namibia), (designation and information are given in Table 1. All non-axenic cultures were kept at 15°C in L1 medium (Guillard and Hargraves, 1993) based on autoclaved seawater with a salinity of 32 and a pH value of 8.1. The L1 growth medium was selected to ensure nutrient-replete conditions during the experiment.

134 **Table 1**: Information on *Pseudo-nitzschia* species and strain designations, sampling location and date, and sources.

Species	Strain	Sampling location	Sampling date	Source
P. australis	IFR-PAU-17	Brest harbor, Brest, France	10/2017	IFREMER, LER-BO, Concarneau, France
P. australis	L3.4	Namibian coasts	12/2016	National Marine Information and Research Centre (NatMIRC), Lüderitz and Swakopmund, Namibia
P. australis	L3	Namibian coasts	12/2016	National Marine Information and Research Centre (NatMIRC), Lüderitz and Swakopmund, Namibia
P. fraudulenta	PNfra 167	Luc sur Mer, English Channel, France	06/2017	UMR BOREA, Normandy university, France
P. fraudulenta	PNfra 169	Luc sur Mer, English Channel, France	06/2017	UMR BOREA, Normandy university, France
P. fraudulenta	IFR-FRA-17	Men Er Roué, Quiberon Bay, France	08/2017	IFREMER, Phycotoxins laboratory, Nantes, France

Experimental set-up

The experiments were carried out at three different pH levels, 8.07 (representing ambient seawater pH level), 7.77 (projected end-of-century seawater pH) and 7.40 (projected pH level by 2300) (Caldeira and Wickett, 2003; IPCC, 2014). The L1 medium was acidified to reach the different pH levels 7.40, 7.77 and 8.07 (corresponding to pCO_2 concentrations of 1845, 783 and 380 ppm, respectively) by CO_2 bubbling (Air Liquid Denmark A/S. UN 1013 Carbon Dioxide, Class 2, 2A, ADR).

The strains of *P. fraudulenta* and *P. australis*, including the two subclones L3-30 and L3-100, were grown in triplicates at the three different pH levels. The cells were acclimated to the different pH treatments for at least 20 generations, and were considered acclimated when growth rates did not vary more than ±0.05 d^{-1} for at least three consecutive generations at each pH condition (Maclntyre and Cullen, 2005). All cells were grown in triplicate semi-continuous cultures in 65 mL Nunclon polystyrene flasks filled up to capacity with L1 medium of the specific pH value. The cultures were diluted daily, and the dilution rate corresponded approximately to the growth rate, where 60% to 90% d^{-1} of the total culture volume was replaced with an equal volume of pH-specific medium. Daily dilutions were employed to keep the cells at low densities (between 500 and 2000 cell mL^{-1}) in order to avoid pH increases during the experimental period (Hansen et al., 2007; Lundholm et al., 2004). Cultures were kept in suspension by agitation on a plankton wheel (1 rpm) in a temperature-controlled room at 15°C, exposed to a photon flux density of 100 µmol photons m^{-2} s^{-1} cool white light following a light: dark cycle of 16: 8 h. The pH level was measured before and after dilution using a WTW pH 340i

156 pH-meter with a SenTix 41 glass electrode, with a sensor detection limit of 0.01. The pH-meter
157 was calibrated daily (2-point calibration) using WTW-pH buffers of pH 7.00 and 10.00.
158 *Growth monitoring*

159 Cell growth was monitored on a daily basis for 14 days by both cell counts (one replicate) and
160 Relative Fluorescence Unit (RFU) measurements (all three replicates). Sub-sampling was carried
161 out at the same time of the day every day. For cell counts, 1 mL samples were fixed with acidic
162 Lugol's solution and a minimum of 400 cells counted using a Nageotte counting chamber and a
163 light microscope Olympus CKX53 at 10× magnification. For RFU measurements, 1 mL was
164 transferred to a quartz cuvette and RFU determined using a Trilogy® laboratory fluorometer
165 (Turner Designs, San Jose, CA, USA). A standard curve for each strain ($r^2 > 0.90$) relating the
166 RFU measurements and the cell counts was used to estimate the cell density for all replicates. For
167 calculation of growth rates, the daily dilutions were taken into consideration. The specific growth
168 rate for the mean value of the triplicates (μ, d^{-1}) was calculated for the last four days of the
169 experiment (when growth rates did not vary more than ± 0.05 d^{-1}) (Guillard, 1973).
170 *Cell volume*
171 For each strain, 50 cells in exponential growth phase were selected and measured using an
172 Olympus BX53 microscope at x100 magnification equipped with an Olympus DP74 digital
173 camera and CellSens imaging software CellSens Entry v1.41. The calculations of cell volume
174 were done at day 0 and 14, and no effect of pH variation on cell volume was observed over the
175 course of the experiment, therefore only the results of the first measurements are shown. Cell
176 volume measurements were calculated for each combination of strain and treatment strain, as

177 mean ± standard deviation of 50 cells with the assumption that the width and thickness of
178 *Pseudo-nitzschia* cells are similar using the following equation (Lundholm et al., 2004).

179 $V = \frac{1}{2} a \times b^2$

180 With a = length, b = width

181 *Nutrient concentrations*

182 Dissolved nutrient concentrations were measured at the beginning and the end of the experiments.
183 Samples (3 × 24 mL) for inorganic nitrate, phosphate and silicate were passed through
184 polycarbonate 0.2 µm filters and stored frozen at -20°C immediately after collection, exept for
185 silicate samples stored at 4°C. Phosphate and silicate samples were analyzed with a Trilogy®
186 laboratory fluorometer (Turner Designs, San Jose, CA, USA) using standard colorimetric
187 techniques (Hansen and Koroleff, 1999). For analyses of inorganic nitrate, samples were analyzed
188 on an ALPKEM auto-analyzer (Solorzano and Sharp, 1980).

189 *Toxin profile (particulate and dissolved)*

190 On the last day of the experiment, 20 mL of exponentially growing culture was sampled for
191 measuring particulate and dissolved DA fractions. Samples were centrifuged (3000 g, 15 min at
192 4°C) and separated into cell pellet and supernatant. The cell pellet was suspended with 1 mL
193 methanol/water mixture (50/50: v/v) to measure particulate DA content. The extraction was
194 prolonged by 15 min of sonication in an ice-cold bath then centrifuged and filtered (8000 g, 15
195 min, 4°C, 0.2 µm) to recover the supernatant and stored at -80°C for later analyses (Calu, 2011).
196 DA content in the dissolved fraction was extracted by solid phase extraction (SPE) using Agilent

197 Bond Elut 200 mg C_{18} cartridges (Ayache et al., 2019). The SPE column was conditioned with 10
198 mL methanol followed by 10 mL high purity water. The sample was acidified with 20% aqueous
199 formic acid (200 µL) then passed through the SPE column. The cartridge was rinsed with 10 mL
200 of 0.2% aqueous formic acid then dried for 1 minute. DA was eluted with 1.5 mL of
201 methanol/water (50/50: v/v) into a glass vial and stored at -80 °C for later analysis.

202 DA analyses were performed using Ultra-Fast Liquid Chromatography (UFLC, Shimadzu)
203 coupled to an ABSciex API 4000 Q-Trap (triple quadrupole mass spectrometer) (Ayache et al.,
204 2019). The chromatographic separation was carried out on a Kinetex C_{18} column (150 × 2.1 mm,
205 2.6 µm, Phenomenex) equipped with a pre-column. A certified DA standard (CNRC, Halifax,
206 Canada) was used for external calibration range in order to quantify DA. The limit of detection
207 (LOD) and limit of quantification (LOQ) were respectively 0.1 and 0.25 ng mL^{-1}. The particulate
208 (pDA) and dissolved DA (dDA) contents were expressed on a per cell basis (pg $cell^{-1}$). Total DA
209 (tDA) is calculated by addition of pDA and dDA.

210 *Dissolved inorganic carbon*

211 The concentration of dissolved inorganic carbon (DIC) in the medium in all three pH treatments
212 was measured in triplicates at the end of the experiment. DIC samples (2 × 12 mL) were
213 preserved with mercuric chloride and stored in airtight borosilicate flasks without headspace (to
214 avoid CO_2 leaking out of the water phase) in the dark at 4°C until measurements. DIC
215 concentrations were measured on 1 ml subsamples using an infrared gas analyzer (ADC 225
216 Mk3, Analytic Development Co. Ltd., Hoddesdon, England) as described in detail elsewhere
217 (Nielsen et al., 2007). The carbon speciation (HCO_3^-, CO_3^{2-} and CO_2* [*includes H_2CO_3 and

218 CO_2]) was calculated from pH and DIC concentration at a temperature of 16°C and salinity 32.
219 Calculations were made using the CO2SYS program and the following available inputs: set of
220 constants: K1, K2 from Mehrbach et al. (1973) refit by Dickson & Millero (1987); $KHSO_4$:
221 Dickson; pH scale: seawater (SW) scale (mol kg^{-1} SW) (Lewis and Wallace, 1998).

222 *Statistical analyses*

223 The experiments were carried out in triplicate and the data presented as mean values ± standard
224 deviation (SD). Statistical differences among growth rates, cell volumes, nutrients concentrations
225 and DA content at the different pH levels were determined using a one-way analysis of variance
226 (ANOVA). A pair-wise Tukey HSD multiple comparisons test was performed to identify
227 differences between pH treatments. All data was normally distributed, as determined by the
228 Shapiro-Wilk test, thus permitting the use of parametric statistical analyses. The level of
229 significance (α) was set to 0.05 for all statistical tests.

230 **1.3 Results**

231 *1.3.1 Effect of pH variation on growth and cell volume*

232 The mean growth rates of the *Pseudo-nitzschia australis* strains (including the two clones L3-30
233 and L3-100) were significantly affected by pH (Fig. 1A, Table S1). In strain L3-30, the mean
234 growth rate was significantly higher at pH 8.07 (2.47 d^{-1}) compared to pH 7.77 (2.33 d^{-1}) and pH
235 7.40 (1.72 d^{-1}) ($p < 0.01$). The highest mean growth rates for strains IFR-PAU-17 and L3-100
236 occurred at pH 7.77, which were not significantly different from their respective mean growth
237 rates at pH 8.07 ($p > 0.05$) (Fig. 1A, Table S1). Growth rates decreased significantly for these
238 three strains (IFR-PAU-17, L3-100 and L 3-30) when pH declined to pH 7.40 ($p < 0.001$) (Fig.

239 1A). Whereas for strain L3.4, a significantly higher growth rate ($p < 0.01$) was observed at pH
240 7.77 in comparison to pH 8.07 (1.65 and 1.43 d^{-1}, respectively), and a continued increase,
241 although not significant ($p > 0.05$), was observed between pH 7.77 and 7.40 (1.72 d^{-1}) (Fig. 1A,
242 Table S1).

243 When comparing growth rates among strains in *P. australis*, the overall highest growth rate was
244 observed for strain L3-30 at pH 8.07 (2.47 d^{-1}), which was 1.4-fold higher than in strain L3-100
245 (1.77 d^{-1}), followed by the strain IFR-PAU-17 grown at the same pH (1.67 d^{-1}) ($p < 0.001$) (Fig.
246 1A, Table S1). The overall lowest growth rate was obtained in strain L3.4 at the same pH, 8.07
247 (1.43 d^{-1}) (Fig. 1A). Hence, intraspecific variation in growth rates of *P. australis* at similar pH
248 conditions was considerable, exhibiting a maximum variation spanning from 1.43 to 2.47 d^{-1} at
249 pH 8.07.

250 In contrast to *P. australis*, the mean growth rates of the three *P. fraudulenta* strains were not
251 significantly affected by the pH level ($p > 0.05$). The growth rates ranged between 1.76 and 1.82
252 d^{-1} in strain IFR-FRA-17, between 2.02 and 2.00 d^{-1} in strain PNfra167 and between 1.79 d^{-1} and
253 1.72 d^{-1} in strain PNfra169, grown at pH 8.07 and 7.77, respectively. All *P. fraudulenta* strains
254 showed lower, but not significantly lower, growth rates at the lowest pH (7.40) (1.72, 1.90 and
255 1.64 d^{-1} for IFR-FRA-17, PNfra167 and PNfra169, respectively) compared to the two other pH
256 levels ($p > 0.05$) (Fig. 1B, Table S1). In *P. fraudulenta*, the highest growth rate was obtained in
257 PNfra167 at pH 8.07 (2.02 d^{-1}) and the lowest in strain PNfra167 at pH 7.40 (1.64 d^{-1}) (Fig. 1B,
258 Table S1). Intraspecific variation in growth rates at the same pH was hence considerably smaller
259 in *P. fraudulenta* than in *P. australis* varying maximally from 1.76 to 2.02 d^{-1} and from 1.43 to
260 2.47 d^{-1} for *P. fraudulenta* and *P. australis* strains, respectively at pH 8.07 (Table S1). In spite of

261 differences among strains, an overall significant negative effect of OA was found on the growth
262 rate of all *P. australis* strains with pH decreasing from 8.07 to 7.40 ($p < 0.005$) and from pH 7.77
263 to 7.40 ($p < 0.05$), whereas, no significant effect of pH changes was detected on *P. fraudulenta*
264 strains.

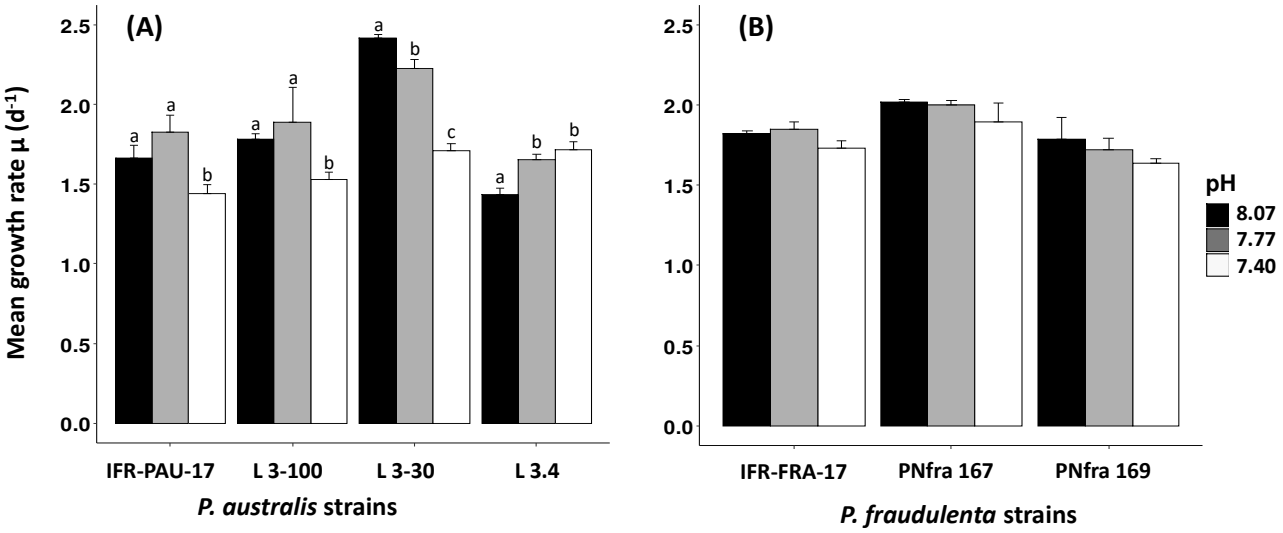

Figure 1: Mean growth rate (d^{-1}) for (A) *P. australis* strains (IFR-PAU-17, L 3.4, L 3-30 and L 3-100) and (B) *P. fraudulenta* strains (IFR-FRA-17, PNfra 167 and PNfra 169) acclimated at three different pH levels (pH= 8.07, 7.77 and 7.40). Error bars represent ± SD, n=3. For each strain, pH treatments with different superscript letters were significantly different.

No effect of pH on the cell volume was observed for all the studied strains. For the *P. australis* strains, the mean cell volumes ranged between 629 μm^3 and 1642 μm^3 and between 660 $\mu m^3$and 1179 μm^3 for the *P. fraudulenta* strains (Fig. 2A and B). The strains of the two species therefore have similar cell volumes. In *P. australis*, the highest cell volume was observed in strain L3-30 (1642 μm^3) which differed significantly ($p < 0.05$) from strains IFR-PAU-17 and L3-100 (1241 and 1112 μm^3, respectively). The lowest cell volume, however, was obtained in L3.4 (627 μm^3), which was significantly lower ($p < 0.05$) than all the other *P. australis* strains (Fig. 2A). The cell volumes of the subclones L3-30 and L3-100 were affected by the culturing history ($p < 0.001$), because the subclone grown at the highest light intensity (L3-100) had a 32% smaller cell volume compared to L3-30 (Fig. 2A). In *P. fraudulenta*, the highest cell volume, obtained in strain IFR-FRA-17 (1179 μm^3), differed significantly from the two other strains PNfra167 and PNfra169, which were not significantly different from each other (696 and 660 μm^3, respectively) ($p > 0.05$) (Fig. 2B).

278

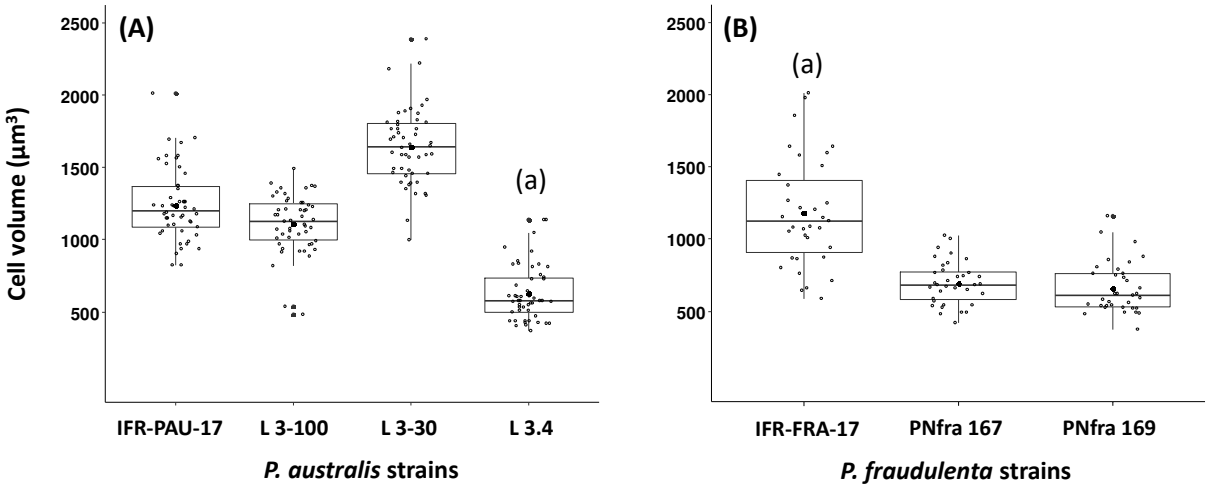

Figure 2: Mean cell volume (µm^3) for (A) *P. australis* strains (IFR-PAU-17, L 3.4, L 3-30 and L 3-100) and (B) *P. fraudulenta* strains (IFR-FRA-17, PNfra 167 and PNfra 169). Error bars represent ± SD, n=50.

(a) Significant difference existed among the mean cell volume of one strain compared to the other strains of the same species ($p < 0.001$).

279 *1.3.2 Measurements of pH, dissolved nutrients and inorganic carbon (DIC) content*

280 The pH in all the experimental treatments fluctuated minimally (< +/- 0.02 units) from the
281 designated pH levels of 8.07, 7.77 and 7.40 throughout the experimental period (Fig. 3).

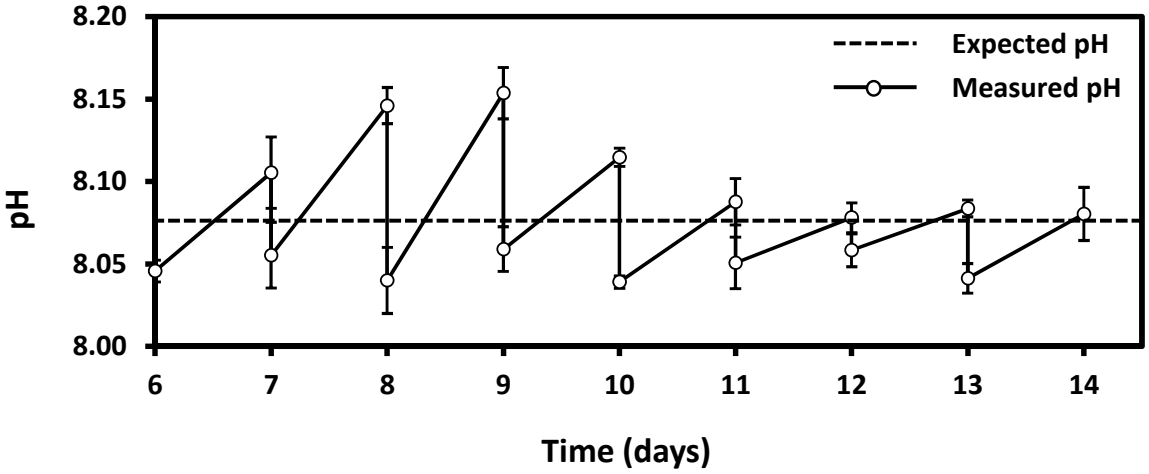

Figure 3: Example of pH adjustments for the culture of *P. australis* IFR-PAU-17 under the pH treatment 8.07. The first days represent the acclimation period and are not included in the results. Error bars represent ± SD, n=3.

282

283 Dissolved nitrogen (N), phosphate (P) and silicate (Si) concentrations were measured in the L1
284 medium prepared for the experiments, and on the last day of sampling. The mean nutrient
285 concentration in all strains acclimated to the different pH levels were equal to 664 µM dissolved
286 N, 33.5 µM dissolved P and 144.8 µM dissolved Si (Table S2), and hence none of the strains
287 were nutrient-limited at any of the pH levels.

The DIC concentrations measured in the *P. australis* strains ranged between 1924 and 2104 µmol L^{-1}, and between 2016 and 2173 µmol L^{-1} for *P. fraudulenta* strains for all pH treatments (Table S3). As expected, the concentrations of HCO_3^-, CO_3^{2-} and CO_2 were significantly different among the pH treatments ($p < 0.05$) (Table S3). In all pH treatments, the carbon speciation of DIC was dominated by bicarbonate ion (HCO_3^-). The concentrations of HCO_3^- (91% to 95%) and CO_2 (1% to 3%) increased with decreasing pH from pH 8.07 to pH 7.40, respectively, whereas the concentration of CO_3^{2-} decreased (8% to 2%) (Table S3).

1.3.3 Effect of pH variation on toxin content

No particulate (pDA) or dissolved domoic acid (dDA) was detected in any of the *P. fraudulenta* strains at a detection limit of 0.1 ng mL^{-1}. The *P. australis* strains confirmed their capability for DA production at all three pH levels (pDA and dDA) (Fig. 4A and B, Table S4). Despite the differences in biovolume among the *P. australis* strains, pDA and dDA contents showed the same trend when expressed per cell and per volume, therefore only content per cell are presented below.

For *P. australis* strain IFR-PAU-17 and the two clones L3-100 and L3-30, particulate DA content was significantly higher ($p < 0.001$) at pH 8.07 relative to pH 7.77 (Fig. 4A), whereas pDA content remained unchanged in strain L3.4 ($p > 0.05$). At the lowest pH 7.40, all strains showed relatively constant cellular DA content relative to pH 7.77 ($p > 0.05$), except for strain IFR-PAU-17. The latter's pDA was significantly higher at pH 7.40 (1.23 pg $cell^{-1}$) than at pH 7.77 (0.25 pg $cell^{-1}$) but still lower than pH 8.07 (2.49 pg $cell^{-1}$) ($p < 0.01$). All strains thus showed lower or unchanged particulate DA content (except for strain IFR-PAU-17) with pH decreasing from 8.07

309 to 7.40 (Table S4). The highest pDA content was detected in IFR-PAU-17 at pH 8.07 (2.49 pg
310 cell^{-1}). The two clones L3-30 and L3-100 showed similar patterns for pDA contents at the three
311 pH treatments (Fig. 4A). The highest pDA content in clone L3-100 (1.64 pg cell^{-1} at pH 8.07),
312 was significantly higher (4-fold) than the pDA content of the clone L3-30 acclimated at the same
313 pH (0.37 pg cell^{-1}). Overall, the lowest pDA content was obtained in strain L3.4 and it did not
314 differ significantly ($p > 0.05$) among the three pH levels tested (ranging between 0.06 and 0.07 pg
315 cell^{-1} at pH 7.40, 7.77 and 8.07) (Fig. 4A, Table S4).

316

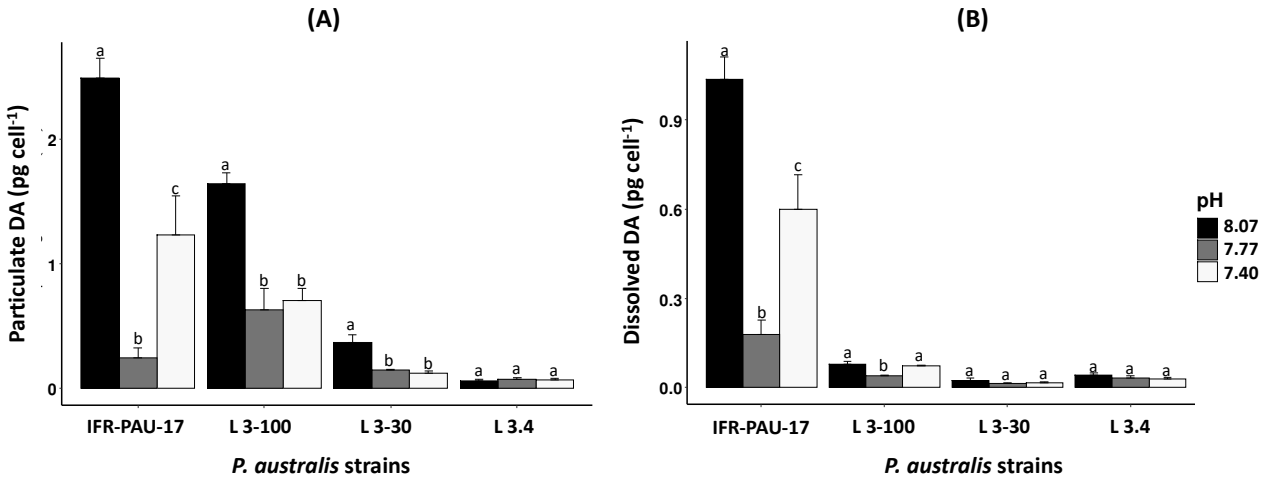

Figure 4: Particulate (A) and dissolved (B) DA contents (pg cell^{-1}) for *P. australis* strains (IFR-PAU-17, L 3.4, L 3-30 and L 3-100) acclimated at three different pH levels (pH= 8.07, 7.77 and 7.40). Data are means ± SD, n=3. For each strain, pH treatments with different superscript letters were significantly different.

317 Similar to pDA, the highest dDA content for all *P. australis* strains was detected at the highest
318 pH treatment 8.07 (Fig. 4B). At this pH, dDA content was significantly higher ($p < 0.001$) in
319 strain IFR-PAU-17 (1.04 pg cell^{-1}) compared to the three other strains L3-100 (13-fold), L3.4
320 (26-fold) and L3-30 (52-fold) at the same pH (Fig. 4B, Table S1). In strains IFR-PAU-17 and L3-
321 100, dDA content was significantly higher at pH 8.07 ($p < 0.001$) compared to the pH level 7.77,
322 whereas in the other two strains there was no significant difference (Fig. 4B). In strain IFR-PAU-
323 17, dDA was significantly higher at pH 7.40 (0.60 pg cell^{-1}) in comparison with pH 7.77 (0.18 pg
324 cell^{-1}) ($p > 0.05$) (Fig. 4B). A similar, but not significant, pattern was seen for strain L3-100 with
325 2-fold increasing dDA levels from pH 7.77 to pH 7.40 (Fig. 4B, Table S4). Whereas strains L3.4
326 and L3-30 did not show any significant differences in dDA content among any of the three pH
327 levels ($p > 0.05$) (Fig. 4B).

328 The overall variations in total cellular content of DA (tDA) were similar to variations in pDA.
329 The highest tDA content was obtained at pH 8.07 for most of the *P. australis* strains IFR-PAU-17
330 (3.53 ± 0.23 pg cell^{-1}), L3-100 (1.72 ± 0.10 pg cell^{-1}) and L3-30 (0.39 ± 0.07 pg cell^{-1}). At pH
331 8.07, strain IFR-PAU-17 produced the highest amount of total DA (3.53 ± 0.23 pg cell^{-1}) (Table
332 S4), while the lowest tDA content was obtained in strain L3.4 (0.10 ± 0.02 pg cell^{-1}) (Table S4).
333 Interestingly, in strains L3.4 and IFR-PAU-17, dissolved DA as a percentage of total DA ranged
334 from 30%-40% for the two species at all three pH levels, whereas the dDA fraction in strains L3-
335 30 and L3-100 represented maximum 7 % of the tDA content at all pH levels with the exception
336 of strain L3-30 at pH 7.40 where the dDA fraction represented 13 % of the total DA content (Fig.
337 5).

338

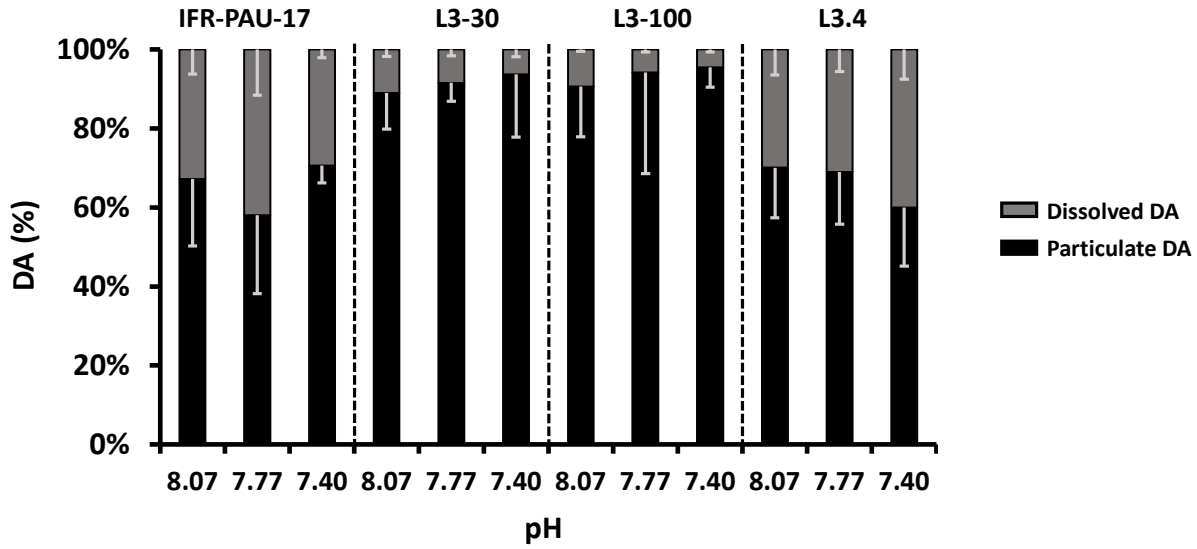

Figure 5: Particulate and dissolved DA expressed as a percentage of total DA at the different pH levels: 8.07, 7.77 and 7.40 in *P. australis* strains (IFR-PAU-17, L 3.4, L 3-30 and L 3-100) Data are means ± SD, n=3.

1.4 Discussion

1.4.1 Effect of pH variation on growth rate

The mean growth rates for two *P. australis* strains (IFR-PAU-17 and L 3-100) did not vary between pH levels 8.07 and 7.77. However, their mean growth rates at pH 7.40 were 11-30% and 19-26% lower compared to what was measured at pH of 8.07 and 7.77, respectively. By contrast, lowering pH from current level (8.07) to predicted pH level in 2100 (7.77) affected other strains either negatively (L3-30) or positively (L3.4). However, there was no statistical variation in growth rate of the three non-toxic *P. fraudulenta* strains grown at pH equal to 8.07, 7.77 and 7.40. Apparently contrasting results were reported for the polar species *Pseudo-nitzchia subcurvata*, where growth rates increased significantly with increased CO_2/lowered pH levels from 205ppm ~ pH 8.31 to 425 ppm ~ pH 8.02 (Zhu et al. (2017). These experiments were, however, performed mainly at CO_2 concentrations lower than current atmospheric levels of ~400 ppm (pH 8.05) and did not explore scenarios of ocean acidification. Similar to our findings, Wingert et al. (2017) reported a decrease in growth rate for an *P. australis* strain cultured at pH 7.8 (0.95 d^{-1}) (ca. 30 % decrease) in comparison with the three higher pH treatments pH 8.1, 8.0 and 7.9 (μ = 1.33, 1.26 and 1.30 d^{-1}, respectively). Moreover, Hancock et al. (2018) and Davidson et al. (2016) found negative effects of high CO_2/low pH on the abundance of *P. subcurvata* in natural communities, as well as in a mixed Antarctic microbial assemblage, respectively. Other studies, including most of our results, hence show a lower growth rate in *Pseudo-nitzschia* with ocean acidification. A possible explanation for the decrease in growth rates with decreasing pH (and increasing in H+ ions) may be linked to potentially more energy spent on maintaining pH homeostasis necessary for cell functioning at the expense of growth in these strains (Beardal and

361 Raven, 2004; Riebesell, 2004; Berge et al.2010), and deviations from optimum intracellular pH of
362 cells may directly affect physiological processes such as enzyme activity, protein function,
363 nutrient uptake (Gattuso and Hansson, 2009; Graneli and Haraldsson, 1993; McMinn et al.,
364 2014).

365 In contrast to the above-mentioned results, a single strain of *P. australis*, L3.4, showed an overall
366 positive effect on growth rate of lower pH conditions (7.40) compared to higher pH (8.07) in the
367 present study (Fig. 1A). Similarly, based on figure-derived rates, a relative increase in growth
368 rates (from 0.4 to 0.7 d^{-1}) were found with increasing pCO_2 (from 220 ppm to 730 ppm
369 corresponding to approximately pH 8.19 and 7.96, respectively) for a *P. multiseries* strain
370 maintained under nutrient-replete conditions (Sun et al., 2011). In addition, in *P. fraudulenta*
371 nutrient-replete cultures, Tatters et al. (2012) also reported a significant progressive increase in
372 growth rates with increasing pCO_2 levels (an increase of 48% and 66% relative to the 200 ppm ~
373 pH 8.43, 360 ~ pH 8.22 and 765 ppm ~ pH 7.95, respectively). Several studies thus also report
374 positive effects on growth rates in *Pseudo-nitzschia* due to experimental OA. Increased
375 concentrations of atmospheric CO_2 from current levels to 700 ppm (~ pH 7.81) has been
376 suggested to generally increase the growth of marine phytoplankton by 40% (Schippers et al.,
377 2004b), especially for species relying on CO_2 or HCO_3^- uptake (Hein and Sand-Jensen, 1997;
378 Riebesell et al., 2007). In *Pseudo-nitzschia* species, *P. multiseries* has been shown to rely almost
379 equally on CO_2 or HCO_3^- uptake (Trimborn et al. 2008); nothing is known for other *Pseudo-*
380 *nitzschia* species. Most phytoplankton species have highly regulated carbon concentrating
381 mechanisms (CCMs), that might allow them to avoid CO_2 limitation and support their
382 photosynthesis productivity at low pCO_2 (high pH) levels (Reinfelder, 2011; Sobrinho et al.,

383 2017; Trimborn et al., 2013). At low pH levels, however, relatively more carbon is available as
384 CO_2 and HCO_3^- and it is not likely that *Pseudo-nitzschia* suffer carbon-limitation. Operating and
385 maintaining CCMs requires cellular energy (ATP), therefore, cells grown at lower pH might use
386 less energy for CCMs and thus have higher growth rates (Hopkinson et al., 2010; Hutchins et al.,
387 2009).

388 The contrasting results observed in our experiment between the tested *P. australis* strains
389 illustrate the need to include multiple strains, and to perform studies on populations (natural or
390 artificial) to understand responses of individual species, and communities, to future OA. For
391 comparison among studies, differences in experimental set-up further complicates conclusions,
392 but even with our relatively restricted number of strains, we saw contrasting results in growth
393 response to OA. This may seem logical, but none the less, deductions based on single strains are
394 often made when considering effects of relevance for HAB blooms or ecosystem effects.

395 *1.4.2 Effect of culturing on growth rate physiology*

396 The two subclones with a different culturing history regarding light intensity had different cell
397 volumes. The differences observed in subclone-specific may be explained by the fact that the
398 growth of unicellular microalgae is inversely proportional to their cell size (Banse, 1976). This
399 was also observed in the present study. The strains with the lowest growth rate, L3-30, showed a
400 rather a higher cell volume compared to small-sized subclone, L3-100, the cell volume of which
401 was ca. 32 % smaller (Fig. 2A). Combining the facts that 1) at higher light intensity, *Pseudo-*
402 *nitzschia* cells have been shown to accelerate their growth rate (Auro and Cochlan, 2013; Pan et
403 al., 1996; Thorel et al., 2014), and 2) that diatom cells are known to gradually decrease in overall

cell size during vegetative reproduction e.g. (Mann, 1988), explains why the subclone grown at high light generally had a smaller cell volume. Therefore, the decrease in growth rate in L3-100 compared to L3-30 may be due to differences in the physiological state of the cells (they are physiologically "older"), as subclone L3-100 was subjected to accelerated division conditions (high light) compared to L3-30 maintained at low light.

1.4.3 Effect of pH variation on particulate and dissolved DA content

As expected, DA was produced by the potentially toxic strains of *P. australis*, while no DA production was found in the strains of *P. fraudulenta*.

The particulate DA content decreased significantly in most of the toxic *P. australis* strains (IFR-PAU-17, L3-30 and L3-100) with pH decreasing from 8.07 to 7.77, and was most pronounced for strain IFR-PAU-17 where the decrease in particulate DA content was almost 10-fold (Fig. 5). In contrast the last strain, L3.4, showed no significant change in particulate DA content.

Only few studies have explored effects of ocean acidification i.e. lowered pH on DA production, having used either a single strain of *Pseudo-nitzschia* or a mixed natural community (Sun et al., 2011; Tatters et al., 2018, 2012; Wingert, 2017; Wohlrab et al., 2020). All studies reported that projected future 2100 levels (pH 7.8-7.9) compared with present day CO_2 /pH levels (pH c. 8.1) resulted in higher DA content, i.e. the opposite result of the present study. Sun et al. (2011) and Tatters et al. (2012) observed an increase in total DA content in treatments combining high pCO2/low pH levels (2100 CO2 levels 800 ppm ~ pH 7.95 compared to current concentrations 360 ppm ~ pH 8.22) with nutrient-limited growth conditions. The authors suggested that higher pCO_2 concentrations induced DA production as a consequence of an excess carbon supply together with phosphorus and silicon-limited treatments for both *P. multiseries* and *P.*

426 *fraudulenta* species, respectively. But under P-replete conditions, Sun et. al. (2011) showed that
427 although total DA did increase by 2-3 fold, the actual DA concentrations were 30-50-fold lower
428 than at similar pH conditions under nutrient-deplete conditions. This is very similar to Wingert et
429 al. (2017) who also only found an increase in total DA content in stationary phase nutrient-
430 limited *P. australis* cells (3 to 4 fold increase in tDA) at pH 7.8 relative to pH 8.1. This higher
431 particulate DA content, was in the latter study associated with the lowest growth rate found at this
432 low pH level and may hence be explained by a slow-down of cell division and hence
433 accumulation of particulate DA in the cells.

434 With respect to natural assemblage experiments, Tatter et al.(2018) found that particulate DA
435 contents increased at lower pH levels (380 vs. 800 ppm CO_2 corresponding to pH 8.22 and 7.95,
436 respectively) for *P. multiseries* cells grown with nitrate as N-source at 19°C, but the exact
437 opposite was found when grown with urea as N-source, and no increases or decreases in DA were
438 found when grown at a higher temperature (23°C). Several factors are thus interacting an
439 affecting DA-production, making final conclusions difficult. More recently, during a mesocosm
440 study, Wohlrab et al. (2020) showed that volumetric DA concentrations increased significantly at
441 higher pCO_2/low pH level (1000 µatm ~ pH 7.66) when inorganic macronutrients (N, P and Si)
442 and diatom abundance were limited at the end of the experiment. The authors suggested that
443 when primary metabolism is decreased by nutrient depletion while photosynthesis persists, the
444 available excess energy/ precursors are favored for the production of secondary metabolites e.g.
445 DA production (Bates et al., 1991; Terseleer et al., 2013; Wohlrab et al., 2020).

446 Another possible explanation for an increase in DA at lower pH (as also observed at pH 7.40 for
447 strain IFR-PAU-17) may result from the physiological stress caused by lowering pH levels below

448 adequate pH conditions, e.g. from changes in cellular enzymatic processes, changes in metal
449 speciation, bacterial community composition shifts, nutrient depletion or modifications in the
450 internal optimum pH for DA production, all factors which have been suggested to affect the
451 production of DA (Lundholm et al. 2004; Tatters et al. 2012).

452 Nutrient depletion was not detected in the present study. The decrease in DA content with
453 decreasing pH that we observed in the present study in contrast to previous studies can be
454 explained by some of the same mechanisms as above but with opposite results for different
455 species. It can on the other hand also be explained by cells being under stress and hence
456 allocating less energy for DA production, and more for maintaining growth and homeostasis. The
457 direct effects of changes in environmental pH on DA content is thus unclear but several studies
458 have suggested that it can be related to the changes in intracellular pH and membrane potential, as
459 well as enzyme activity, all of which could influence cell metabolism (Lundholm et al., 2004;
460 Beardal and Raven, 2004; Giordano et al., 2005; Trimborn et al., 2008).

461 The particulate DA content of the two subclones (L3-30 and L3-100) showed similar patterns at
462 the three different pH treatments, but with much lower DA content in L3-30 (e.g. 77% lower at
463 pH 8.07). This variability in DA content may be attributed to the differences in growth rate,
464 assuming that the DA production rates are the same in the two subclones. The faster growing
465 clone, L3-30, had a lower DA content because of DA "dilution" in the cells caused by a faster
466 cell division.

467 The variability in toxin content among the *P. australis* strains seen in the present study
468 emphasizes the difficulties in comparing results from different studies using different strains, and

469 in deriving conclusions about physiological behavior like toxin production and growth response
470 using a single strain. Many physiological studies are still performed based on only one strain,
471 most likely because use of multiple strains multiplies the experimental effort and restricts
472 exploring multiple factors.

473 **1.5 Conclusion**

474 Overall, *P. fraudulenta* and most of *P. australis* strains showed capacity to acclimate and exhibit
475 similar growth rates when comparing current pH (8.07) and projected pH in 2100 (7.80),
476 indicating that these strains may not be affected by ongoing ocean acidification, although daily
477 pH variations due to photosynthesis and respiration processes should be considered, especially as
478 a further decrease in pH (7.40) resulted in a significant reduction in the growth rate of most of *P.*
479 *australis* strains. OA will "demand" that the cells are able to cope with even larger variations in
480 future water pH, as pH will change from a low OA-induced pH to a high pH during bloom
481 periods.

482 For most of the *P. australis* strains, DA content was highest in cultures acclimated at the ambient
483 pH (8.07), and lowest at the projected 2100 seawater pH (7.77). This was however in contrast to
484 most other studies, and thus makes it difficult to predict whether toxicity of *P. auatralis* will
485 present a lower or a higher risk for DA accumulation in a future affected by OA.

486 The diversity in the physiological responses highlights a strong inter- and intra-specific variation
487 in *Pseudo-nitzschia*, and suggests use of multiple strains in future studies. Furthermore, it
488 highlights that the culturing history (e.g. effect of different light intensities) of strains may affect

the physiology, an issue that needs future attention, as it may affect deductions from laboratory studies to field scenarios.

Acknowledgements

The authors acknowledge Ifremer and the Regional Council of the "Région *des Pays de la Loire"* for the PhD funding of Nour Ayache. The authors would like to thank Audrey Duval and Nicolas Chomérat from Ifremer, Concarneau, France for providing and identifying the French *Pseudo-nitzschia australis* IFR-PAU-17 strain, and Deon Louw and Cecilie Hedemand for providing the Namibian *Pseudo-nitzschia australis* L3-100, L3.4 and L3-30 strains. Thanks are also due to Juliette Fauchot from UMR BOREA, Normandy University, France, for providing the two *P. fraudulenta* strains PNfra167 and PNfra169. The authors thank Georges-Augustin Rovillon for his invaluable help for technical assistance in toxin analysis.

References

Auro, M.E., Cochlan, W.P., 2013. Nitrogen Utilization and Toxin Production by Two Diatoms of the Pseudo-nitzschia pseudodelicatissima Complex: P. cuspidata and P. fryxelliana. J. Phycol. 49, 156–169. https://doi.org/10.1111/jpy.12033

Ayache, N., Hervé, F., Martin-Jézéquel, V., Amzil, Z., Caruana, A.M.N., 2019. Influence of sudden salinity variation on the physiology and domoic acid production by two strains of Pseudo-nitzschia australis. J. Phycol. 195, 186–195. https://doi.org/10.1111/jpy.12801

Banse, K., 1976. Algal cell size and the maximum density and biomass of phytoplankton. Limnol. Oceanogr. 32, 983–986.

Bates, S.S., de Freitas, A.S.W., Miley, J.E., Pocklington, R., Quilliam, M.A., Smith, J.C., Worms, J., 1991. Controls on domoic acid production by the diatom Nitzschia pungens f. multiseries in culture: nutrients and irradiance. Can. J. Fish. Aquat. Sci. 48, 1136–44.

Bates, S.S., Hubbard, K.A., Lundholm, N., Montresor, M., Leaw, C.P., 2018. Pseudo-nitzschia, Nitzschia, and domoic acid: New research since 2011. Harmful Algae 79, 3–43. https://doi.org/10.1016/j.hal.2018.06.001

Beardal, J., Raven, J., 2004. The potential effects of global climate change on microalgal photosynthesis, growth and ecology. Phycologia 43, 26–40.

Berge, T., Daugbjerg, N., Andersen, B.B., Hansen, P.J., 2010. Effect of lowered pH on marine phytoplankton growth rates. Mar. Ecol. Prog. Ser. 416, 79–91. https://doi.org/10.3354/meps08780

Caldeira, K., Wickett, M.E., 2003. Anthropogenic carbon and ocean pH. Nature 425, 365. https://doi.org/10.1038/425365a

Calu, G., 2011. Contribution to the study of Pseudo-nitzschia toxicity: regulation of domoic acid production and synthesis of chemical analogues. Nantes, France.

Cho, E.S., Kotaki, Y., Park, J.G., 2001. The comparaison netween toxic Pseudo-nitzschia multiseries (Hasle) Hasle and non-toxic P. pungens (Grunow) Hasle isolated from Jinhae Bay, Korea. Algae 16, 275–285.

Cornwall, C.E., Hepburn, C.D., McGraw, C.M., Currie, K.I., Pilditch, C.A., Hunter, K.A., Boyd, P.W., Hurd, C.L., 2013. Diurnal fluctuations in seawater pH influence the response of a calcifying macroalga to ocean acidification. Proceedings. Biol. Sci. 280, 20132201. https://doi.org/10.1098/rspb.2013.2201

Davidson, A.T., McKinlay, J., Westwood, K., Thomson, P.G., Van Den Enden, R., De Salas, M., Wright, S., Johnson, R., Berry, K., 2016. Enhanced CO2 concentrations change the structure of Antarctic marine microbial communities. Mar. Ecol. Prog. Ser. 552, 93–113. https://doi.org/10.3354/meps11742

Di Liberto, T., 2015. California closes Dungeness and razor clam fisheries due to algal toxin

536 [WWW Document]. NOAA Clim. URL https://www.climate.gov/news-features/event-
537 tracker/california-closes-dungeness-and-razor-clam-fisheries-due-algal-toxin (accessed
538 5.18.20).

539 Dickson, A.G., Millero, F.J., 1987. A comparison of the equilibrium constants for the dissociation
540 of carbonic acid in seawater media. Deep Sea Res. Part A, Oceanogr. Res. Pap. 34, 1733–
541 1743. https://doi.org/10.1016/0198-0149(87)90021-5

542 Doney, S.C., 2010. The growing human footprint on coastal and open-ocean biogeochemistry.
543 Science (80-.). 328, 1512–1513. https://doi.org/10.1016/S0140-6736(16)32143-2

544 Feely, R.A., Sabine, C.L., Hernandez-ayon, J.M., Ianson, D., Hales, B., 2008. Evidence for
545 Upwelling of Corrosive Continental "Acidified"water onto the continental Shelf. Science
546 (80-.). 1490, 1–4. https://doi.org/10.1126/science.1155676

547 Flynn, K.J., Blackford, J.C., Baird, M.E., Raven, J.A., Clark, D.R., Beardall, J., Brownlee, C.,
548 Fabian, H., Wheeler, G.L., 2012. Changes in pH at the exterior surface of plankton with
549 ocean acidification. Nat. Clim. Chang. 2, 510–513. https://doi.org/10.1038/nclimate1489

550 Flynn, K.J., Clark, D.R., Mitra, A., Fabian, H., Hansen, P.J., Glibert, P.M., Wheeler, G.L.,
551 Stoecke, D.K., Blackford, J.C., Brownlee, C., 2015. Ocean acidification with
552 (de)eutrophication will alter future phytoplankton growth and succession. Proc. R. Soc. B
553 Biol. Sci. 282, 2–7. https://doi.org/10.1098/rspb.2014.2604

554 Gattuso, J.-P., Hansson, L., 2009. Ocean acidification : background and history, in: Gattuso, J.-P.,
555 Hansson, L. (Eds.), Ocean Acidification. pp. 1–20.

556 Goldstein, T., Mazet, J.A.K., Zabka, T.S., Langlois, G., Colegrove, K.M., Silver, M., Bargu, S.,
557 Van Dolah, F., Leighfield, T., Conrad, P.A., Barakos, J., Williams, D.C., Dennison, S.,
558 Haulena, M., Gulland, F.M.D., 2008. Novel symptomatology and changing epidemiology of
559 domoic acid toxicosis in California sea lions (Zalophus californianus): An increasing risk to
560 marine mammal health. Proc. R. Soc. B Biol. Sci. 275, 267–276.
561 https://doi.org/10.1098/rspb.2007.1221

562 Graneli, E., Haraldsson, C., 1993. Can increased leaching of trace-metals from acidified areas
563 influence phytoplankton growth in coastal waters. Ambio 22, 308–311.

564 Guillard, R.R.L., 1973. Methods for microflagellates and nanno- plankton, in: Stein, J. (Ed.),
565 Handbook of Phycological Methods. Culture Methods and Growth Measurements.
566 Cambridge University Press, New York, pp. 289–312.

567 Guillard, R.R.L., Hargraves, P.E., 1993. Stichochrysis immobilis is a diatom, not a chrysophyte.
568 Phycologia 32, 234–236. https://doi.org/10.2216/i0031-8884-32-3-234.1

569 Hancock, A.M., Davidson, A.T., Mckinlay, J., Mcminn, A., Schulz, K.G., Van Den Enden, R.L.,
570 2018. Ocean acidification changes the structure of an Antarctic coastal protistan community.
571 Biogeosciences 15, 2393–2410. https://doi.org/10.5194/bg-15-2393-2018

572 Hansen, H.P., Koroleff, F., 1999. Determination of nutrients, in: Grasshoff, K., Kremling, K.,

573 Ehrhardt, M. (Eds.), Methods of Seawater Analysis, Third Edition. Verlag Chemie,
574 Germany, pp. 159–228.

575 Hansen, J., Sato, M., Kharecha, P., Russell, G., Lea, D.W., Siddall, M., 2007. Climate change and
576 trace gases. Philos. Trans. R. Soc. 365, 1925–1954. https://doi.org/10.1098/rsta.2007.2052

577 Hein, M., Sand-Jensen, K., 1997. CO2 increases oceanic primary production [6]. Nature.
578 https://doi.org/10.1038/41457

579 Hopkinson, B.M., Xu, Y., Shi, D., McGinn, P.J., Morel, F.M.M., 2010. The effect of CO2 on the
580 photosynthetic physiology of phytoplankton in the Gulf of Alaska. Limnol. Oceanogr. 55,
581 2011–2024. https://doi.org/10.4319/lo.2010.55.5.2011

582 Hutchins, D., Mulholland, M., Fu, F., 2009. Nutrient cycles and marine microbes in a CO2-
583 enriched ocean. Oceanography 22, 128–145. https://doi.org/10.5670/oceanog.2009.103

584 IPCC, 2014. International Governmental Panel on Climate Change (IPCC), Synthesis Report.
585 Contribution of Working Groups I, II and III to the Fifth Assessment Report of the
586 Intergovernmental Panel on Climate Change. R.K. Pachauri and L.A. Meyer, Geneva,
587 Switzerland.

588 Kroeker, K.J., Kordas, R.L., Crim, R., Hendriks, I.E., Ramajo, L., Singh, G.S., Duarte, C.M.,
589 Gattuso, J.P., 2013. Impacts of ocean acidification on marine organisms: Quantifying
590 sensitivities and interaction with warming. Glob. Chang. Biol. 19, 1884–1896.
591 https://doi.org/10.1111/gcb.12179

592 Le Quéré, C., Andrew, R.M., Friedlingstein, P., Sitch, S., Pongratz, J., Manning, A.C.,
593 Korsbakken, J.I., Peters, G.P., Canadell, J.G., Jackson, R.B., Boden, T.A., Tans, P.P.,
594 Andrews, O.D., Arora, V.K., Bakker, D.C.E., Barbero, L., Becker, M., Betts, R.A., Bopp,
595 L., Chevallier, F., Chini, L.P., Ciais, P., Cosca, C.E., Cross, J., Currie, K., Gasser, T., Harris,
596 I., Hauck, J., Haverd, V., Houghton, R.A., Hunt, C.W., Hurtt, G., Ilyina, T., Jain, A.K.,
597 Kato, E., Kautz, M., Keeling, R.F., Klein Goldewijk, K., Körtzinger, A., Landschützer, P.,
598 Lefèvre, N., Lenton, A., Lienert, S., Lima, I., Lombardozzi, D., Metzl, N., Millero, F.,
599 Monteiro, P.M.S., Munro, D.R., Nabel, J.E.M.S., Nakaoka, S.-I., Nojiri, Y., Padin, X.A.,
600 Peregon, A., Pfeil, B., Pierrot, D., Poulter, B., Rehder, G., Reimer, J., Rödenbeck, C.,
601 Schwinger, J., Séférian, R., Skjelvan, I., Stocker, B.D., Tian, H., Tilbrook, B., Tubiello,
602 F.N., Van Der Laan-Luijkx, I.T., Van Der Werf, G.R., Van Heuven, S., Viovy, N.,
603 Vuichard, N., Walker, A.P., Watson, A.J., Wiltshire, A.J., Zaehle, S., Zhu, D., 2018. Global
604 carbon budget 2017. Earth Syst. Sci. Data 10, 405–448. https://doi.org/10.5194/essd-10-405-
605 2018

606 Lefebvre, K.A., Frame, E.R., Kendrick, P.S., 2012. Domoic acid and fish behavior: A review.
607 Harmful Algae 13, 126–130. https://doi.org/10.1016/j.hal.2011.09.011

608 Lewis, E., Wallace, D.W.R., 1998. Program developed for CO2 system calculations,
609 ORNL/CDIAC-105, Carbon Dioxide Information Analysis Center. Oak Ridge, Tennesse.
610 https://doi.org/4735

611 Lundholm, N., Hansen, P.J., Kotaki, Y., 2004. Effect of pH on growth and domoic acid
612 production by potentially toxic diatoms of the genera Pseudo-nitzschia and Nitzschia. Mar.
613 Ecol. Prog. Ser. 273, 1–15. https://doi.org/10.3354/meps273001

614 Maclntyre, H.L., Cullen, J.J., 2005. Using cultures to investigate the physiological ecology of
615 microalgae, in: Andersen, R.A. (Ed.), Algal Culturing Techniques. Elsevier academic press,
616 Burlington, MA, USA, pp. 287–326.

617 Malviya, S., Scalco, E., Audic, S., Vincent, F., Veluchamy, A., Poulain, J., Wincker, P., Iudicone,
618 D., de Vargas, C., Bittner, L., Zingone, A., Bowler, C., 2016. Insights into global diatom
619 distribution and diversity in the world's ocean. Proc. Natl. Acad. Sci. U. S. A. 113, 1516–
620 1525. https://doi.org/10.1073/pnas.1509523113

621 Mann, D.G., 1988. Why didn't Lund see sex in Asterionella? A discussion of the diatom life
622 cycle in nature, in: Round, F. (Ed.), Biopress. Bristol, pp. 385–412.

623 McCabe, R.M., Hickey, B.M., Kudela, R.M., Lefebvre, K.A., Adams, N.G., Bill, B.D., Gulland,
624 F.M.D., Thomson, R.E., Cochlan, W.P., Trainer, V.L., 2016. An unprecedented coastwide
625 toxic algal bloom linked to anomalous ocean conditions. Geophys. Res. Lett. 43, 10,366-
626 10,376. https://doi.org/10.1002/2016GL070023

627 McMinn, A., Muller, M.N., Mertin, A., Ryan, K.G., 2014. The Response of antarctic sea ice
628 algae to changes in pH and CO2. PLoS One 9, e86984. https://doi.org/10.1371/Citation

629 Mehrbach, C., Culberson, C.H., Hawley, J.E., Pytkowicx, R.M., 1973. Measurement of the
630 apparent dissociation constants of carbonic acid in seawater at atmospheric pressure.
631 Limnol. Oceanogr. 18, 897–907. https://doi.org/10.4319/lo.1973.18.6.0897

632 Middelboe, A.L., Hansen, P.J., 2007. High pH in shallow water macroalgal habitats. Mar. Ecol.
633 Prog. Ser. 338, 107–117. https://doi.org/10.2307/24871746

634 Nielsen, L.T., Lundholm, N., Hansen, P.J., 2007. Does irradiance influence the tolerance of
635 marine phytoplankton to high pH? Mar. Biol. Res. 3, 446–453.
636 https://doi.org/10.1080/17451000701711820

637 Orr, J.C., Fabry, V.J., Aumont, O., Bopp, L., Doney, S.C., Feely, R.A., Gnanadesikan, A.,
638 Gruber, N., Ishida, A., Joos, F., Key, R.M., Lindsay, K., Maier-Reimer, E., Matear, R.,
639 Monfray, P., Mouchet, A., Najjar, R.G., Plattner, G.K., Rodgers, K.B., Sabine, C.L.,
640 Sarmiento, J.L., Schlitzer, R., Slater, R.D., Totterdell, I.J., Weirig, M.F., Yamanaka, Y.,
641 Yool, A., 2005. Anthropogenic ocean acidification over the twenty-first century and its
642 impact on calcifying organisms. Nature 437, 681–686. https://doi.org/10.1038/nature04095

643 Pan, Y., Subba Rao, D. V., Mann, K.H., 1996. Acclimation to low light intensity in
644 photosynthesis and growth of Pseudo-nitzschia multiseries Hasle, a neurotoxigenic diatom.
645 J. Plankton Res. 18, 1427–1438. https://doi.org/10.1093/plankt/18.8.1427

646 Reinfelder, J.R., 2011. Carbon Concentrating Mechanisms in Eukaryotic Marine Phytoplankton.
647 https://doi.org/10.1146/annurev-marine-120709-142720

Riebesell, U., 2004. Effects of CO2 enrichment on marine phytoplankton. J. Oceanogr. 60, 719–729. https://doi.org/10.1007/s10872-004-5764-z

Riebesell, U., Schulz, K.G., Bellerby, R.G.J., Botros, M., Fritsche, P., Meyerhöfer, M., Neill, C., Nondal, G., Oschlies, A., Wohlers, J., Zöllner, E., 2007. Enhanced biological carbon consumption in a high CO2 ocean. Nature 450, 545–548. https://doi.org/10.1038/nature06267

Rost, B., Zondervan, I., Wolf-Gladrow, D., 2008. Sensitivity of phytoplankton to future changes in ocean carbonate chemistry: current knowledge, contradictions and research directions. Mar. Ecol. Prog. Ser. 373, 227–237. https://doi.org/10.3354/meps07776

Schippers, P., Lürling, M., Scheffer, M., 2004a. Increase of atmospheric CO2 promotes phytoplankton productivity. Ecol. Lett. 7, 446–451. https://doi.org/10.1111/j.1461-0248.2004.00597.x

Schippers, P., Lürling, M., Scheffer, M., 2004b. Increase of atmospheric CO2 promotes phytoplankton productivity. Ecol. Lett. 7, 446–451. https://doi.org/10.1111/j.1461-0248.2004.00597.x

Scholin, C.A., Gulland, F., Doucette, G.J., Benson, S., Busman, M., Chavez, F.P., Cordaro, J., DeLong, R., De Vogelaere, A., Harvey, J., Haulena, M., Lefebvre, K., Lipscomb, T., Loscutoff, S., Lowenstine, L.J., Marin, R., Miller, P.E., McLellan, W.A., Moeller, P.D.R., Powell, C.L., Rowles, T., Silvagni, P., Silver, M., Spraker, T., Trainer, V., Van Dolah, F.M., 2000. Mortality of sea lions along the central California coast linked to a toxic diatom bloom. Nature 403, 80–84. https://doi.org/10.1038/47481

Sobrinho, B.F., De Camargo, L.M., Sandrini-Neto, L., Kleemann, C.R., Da Costa Machado, E., Mafra, L.L., 2017. Growth, toxin production and allelopathic effects of Pseudo-Nitzschia multiseries under Iron-enriched conditions. Mar. Drugs 15, 331. https://doi.org/10.3390/md15100331

Solorzano, L., Sharp, J.H., 1980. Determination of total dissolved nitrogen in natural waters. Limnol. Oceanogr. 25, 751–754.

Sun, J., Hutchins, D.A., Feng, Y., Seubert, E.L., Caron, D.A., Fu, F.X., 2011. Effects of changing pCO2 and phosphate availability on domoic acid production and physiology of the marine harmful bloom diatom Pseudo-nitzschia multiseries. Limnol. Oceanogr. 56, 829–840. https://doi.org/10.4319/lo.2011.56.3.0829

Tatters, A.O., Fu, F.-X., Hutchins, D.A., 2012. High CO2 and silicate limitation synergistically increase the toxicity of Pseudo-nitzschia fraudulenta. PLoS One 7, e32116. https://doi.org/10.1371/journal.pone.0032116

Tatters, A.O., Schnetzer, A., Xu, K., Walworth, N.G., Fu, F., Spackeen, J.L., Sipler, R.E., Bertrand, E.M., McQuaid, J.B., Allen, A.E., Bronk, D.A., Gao, K., Sun, J., Caron, D.A., Hutchins, D.A., 2018. Interactive effects of temperature, CO 2 and nitrogen source on a coastal California diatom assemblage. J. Plankton Res. 40, 151–164.

https://doi.org/10.1093/plankt/fbx074

Terseleer, N., Gypens, N., Lancelot, C., 2013. Factors controlling the production of domoic acid by Pseudo-nitzschia (Bacillariophyceae): A model study. Harmful Algae 24, 45–53. https://doi.org/10.1016/j.hal.2013.01.004

Thorel, M., Fauchot, J., Morelle, J., Raimbault, V., Le Roy, B., Miossec, C., Kientz-Bouchart, V., Claquin, P., 2014. Interactive effects of irradiance and temperature on growth and domoic acid production of the toxic diatom Pseudo-nitzschia australis (Bacillariophyceae). Harmful Algae 39, 232–241. https://doi.org/10.1016/J.HAL.2014.07.010

Trainer, V.L., Bates, S.S., Lundholm, N., Thessen, A.E., Cochlan, W.P., Adams, N.G., Trick, C.G., 2012. Pseudo-nitzschia physiological ecology, phylogeny, toxicity, monitoring and impacts on ecosystem health. Harmful Algae 14, 271–300. https://doi.org/10.1016/j.hal.2011.10.025

Trimborn, S., Brenneis, T., Sweet, E., Rost, B., 2013. Sensitivity of Antarctic phytoplankton species to ocean acidification: Growth, carbon acquisition, and species interaction. Limnol. Oceanogr. 58, 997–1007. https://doi.org/10.4319/lo.2013.58.3.0997

Trimborn, S., Lundholm, N., Thoms, S., Richter, K.U., Krock, B., Hansen, P.J., Rost, B., 2008. Inorganic carbon acquisition in potentially toxic and non-toxic diatoms: The effect of pH-induced changes in seawater carbonate chemistry. Physiol. Plant. 133, 92–105. https://doi.org/10.1111/j.1399-3054.2007.01038.x

Wingert, C.., 2017. The effects of ocean acidification on growth, photosynthesis, and domoic acid production by the toxigenic diatom, Pseudo-nitzschia australis.

Wohlrab, S., John, U., Klemm, K., Eberlein, T., Forsberg Grivogiannis, A.M., Krock, B., Frickenhaus, S., Bach, L.T., Rost, B., Riebesell, U., Van de Waal, D.B., 2020. Ocean acidification increases domoic acid contents during a spring to summer succession of coastal phytoplankton. Harmful Algae 92, 101697. https://doi.org/10.1016/j.hal.2019.101697

Zhu, Z., Qu, P., Gale, J., Fu, F., Hutchins, D.A., 2017. Individual and interactive effects of warming and CO 2 on Pseudo-nitzschia subcurvata and Phaeocystis antarctica, two dominant phytoplankton from the Ross Sea, Antarctica. Biogeosciences 14, 5281–5295. https://doi.org/10.5194/bg-14-5281-2017